ADVANCED MATERIALS INTERFACES

www.advmatinterfaces.de

Nanostructured CaF_2:Ln^{3+} (Ln^{3+} = Yb^{3+}/Er^{3+}, Yb^{3+}/Tm^{3+}) Thin Films: MOCVD Fabrication and Their Upconversion Properties

Anna L. Pellegrino, Paolo Cortelletti, Marco Pedroni, Adolfo Speghini, and Graziella Malandrino**

Dedicated to Professor Michael Hitchman on the occasion of his 75th birthday

Calcium fluoride represents one of the most efficient hosts for up-conversion or down-conversion emissions. A simple metal organic chemical vapor deposition approach is applied to the fabrication of CaF_2 nanostructured thin films using the fluorinated "second-generation" β-diketonate compound $Ca(hfa)_2$•diglyme•H_2O as a Ca-F single-source precursor. The versatility of the process is demonstrated for the fabrication of up-converting Yb/Er or Yb/Tm codoped CaF_2 films on Si, quartz, and glass substrates. The $Ln(hfa)_3$•diglyme (Ln = Tm, Er, Yb) precursors are used as sources of the doping ions. Structural, morphological, and compositional characterization of the films shows the formation of polycrystalline CaF_2 films with a very uniform surface and suitable doping. In fact, an appropriate tuning of the mixture composition, i.e., the Ca:Ln ratio in the multicomponent source, permits the deposition of films with the desired stoichiometry. The films show promising up-conversion properties in the visible and near infrared regions upon laser excitation for both doping mixtures.

Alkaline earth fluoride materials have attracted great attention due to a wide variety of applications in dielectrics, optics, optoelectronics, and photonics.[1–8] In particular, calcium fluoride has been regarded as one of the most efficient hosts for upconversion (UC) or downconversion emissions, also due to its low phonon energy, which minimizes nonradiative de-excitation processes.[9–15] UV–vis or NIR–vis energy conversion could enhance the efficiency of photovoltaic devices since it makes it possible to collect the radiation energy outside the absorption range of the photoactive material (usually silicon) by shifting its energy to a more suitable optical region. In addition, rare-earth doped CaF_2 compounds are promising luminescent materials as phosphors and in technological applications as micro- and nanoscale thermometry for microelectronics and for biomedical assays.[4,16–18]

A comment deserves the CaF_2 structure, also in view of similar ionic size of the trivalent lanthanide ions, inserted as dopants, and the Ca^{2+} ion. Calcium fluoride has the typical fluorite structure, following the name (fluorite) of the mineral form of CaF_2, which is a simple cubic arrangement of anions with 50% cubic sites filled with Ca^{2+}. Thus, in this structure, calcium is eight coordinated by fluoride ions, a coordination environment suitable for the lanthanide ions, being eight one of the most common coordination number for lanthanides.[19]

Most of the above-mentioned applications require the calcium fluoride material in the form of thin films. Several studies are available on the deposition of CaF_2 thin films using physical vapor deposition techniques, such as sputtering,[20,21] electron beam evaporation,[22] pulsed laser deposition,[23,24] and molecular beam epitaxy.[25,26] Calcium fluoride films have also been deposited through sol–gel chemical routes using spin coating[27] or dip coating.[28] Among the chemical vapor deposition approaches, atomic layer deposition has been applied to the deposition of CaF_2 films.[29]

Nevertheless, even though various deposition methods have been applied to the fabrication of CaF_2 films, a more versatile, easily scalable, fast, and industrially appealing approach is highly desirable.

The metal organic chemical vapor deposition (MOCVD) has the potential advantage of being a very reliable and reproducible method for the fast production of films with high uniformity degree in both thickness and composition over large areas. In addition, note that in the case of potential integration of these layers in photovoltaic cell production, plasma-enhanced CVD is the most common fabrication method for thin film Si-based cells.[30]

A. L. Pellegrino, Prof. G. Malandrino
Dipartimento di Scienze Chimiche
Università di Catania and INSTM UdR Catania
V.le A. Doria 6, 95125 Catania Italy
E-mail: gmalandrino@unict.it
P. Cortelletti, Dr. M. Pedroni, Prof. A. Speghini
Nanomaterials Research Group
Dipartimento di Biotecnologie
Università di Verona and INSTM UdR Verona
Strada le Grazie 15, 37134 Verona, Italy
E-mail: adolfo.speghini@univr.it

The ORCID identification number(s) for the author(s) of this article can be found under https://doi.org/10.1002/admi.201700245.

DOI: 10.1002/admi.201700245

MOCVD has been already applied to the deposition of the fluorite films; nevertheless, most of these reports used a fluorine-free calcium source, thus a second precursor is needed as the fluorine source. The first report on the deposition of CaF_2 with MOCVD dates back to 1989 when the bis(pentamethyl-cyclopentadienyl)calcium was applied as calcium source together with SiF_4 or NF_3 as the fluorine source.[31] More recently, fluorine free β-diketonate has been applied as calcium source combined with the use of ammonium hydrogen fluoride as the fluorine source.[32] A few reports are described in the application of fluorinated precursors to the fabrication of thin films where polyether adducts of the Ca bis-hexafluoroacetylacetonate have been applied, namely, the $Ca(hfa)_2$•tetraglyme[33] and the $Ca(hfa)_2$•diglyme•H_2O.[34–36]

In this study, we report for the first time the synthesis of CaF_2 films doped with Yb^{3+},Er^{3+} or Yb^{3+},Tm^{3+} through a simple MOCVD route on various substrates using a molten mixture consisting of the $Ca(hfa)_2$•diglyme•H_2O and the suitable $Ln(hfa)_3$•diglyme [Ln = Yb, Er, Tm; Hhfa = 1,1,1,5,5,5-hexafluoro-2,4-pentanedione; diglyme = bis(2-methoxyethyl)ether] precursors in an appropriate stoichiometric ratio.

The advantages of the present approach are various: (i) the metal precursors represent also a source of fluorine, thus avoiding the use of harmful hydrogen fluoride (HF) or other fluorine sources during the deposition step; (ii) the application of all the required metal precursors in a unique multicomponent mixture allows for an easy control of the precursor source by simply adjusting the stoichiometric ratio; and (iii) the use of the same polyether (diglyme) to complete the coordination sphere of calcium and lanthanide ions avoids the undesirable potential ligand exchange.

The structural, morphological, compositional, and luminescent properties point to the formation of good quality CaF_2 films with promising upconversion properties reflecting the correct stoichiometry of the films.

The films were deposited on glass, quartz, and Si (100) substrates. Given the same nature of the ligand and similar vaporization temperature ranges of the single precursors,[19,35,36] no ligand exchange occurs and an efficient vaporization without thermal degradation takes place.

The X-ray diffraction (XRD) analysis of the samples CaF_2:Yb 18%, Er 2% (mol % with respect to the total metal content) deposited at 500 °C on Si (100) (**Figure 1)** exhibits patterns associated with a cubic CaF_2 phase (ICDD No. 35-0816). The diffraction features observed at 2θ values of 28.25°, 32.75°, 47.00°, and 55.75° are associated with the 111, 200, 220, and 311 reflections, respectively. The XRD measurements of films deposited at lower and higher temperatures and on different substrates show similar patterns. A closer look to the patterns, recorded with a 0.02° resolution, of films containing different amounts of Yb^{3+} ions reveals a small shift of the peak positions with respect to those found for the undoped CaF_2 film. In Figure 1b, a magnification of the 220 reflection is reported. The red line indicates the position of the ICDD CaF_2 220 peak; a slight shift toward higher angles is found for all the Yb^{3+} doped CaF_2 films. This behavior may be correlated on the one side to the ionic radii of the involved doping ions and on the other hand to the need of charge balance due to the different charge 2+ of Calcium and 3+ of lanthanide ions, which can be compensated

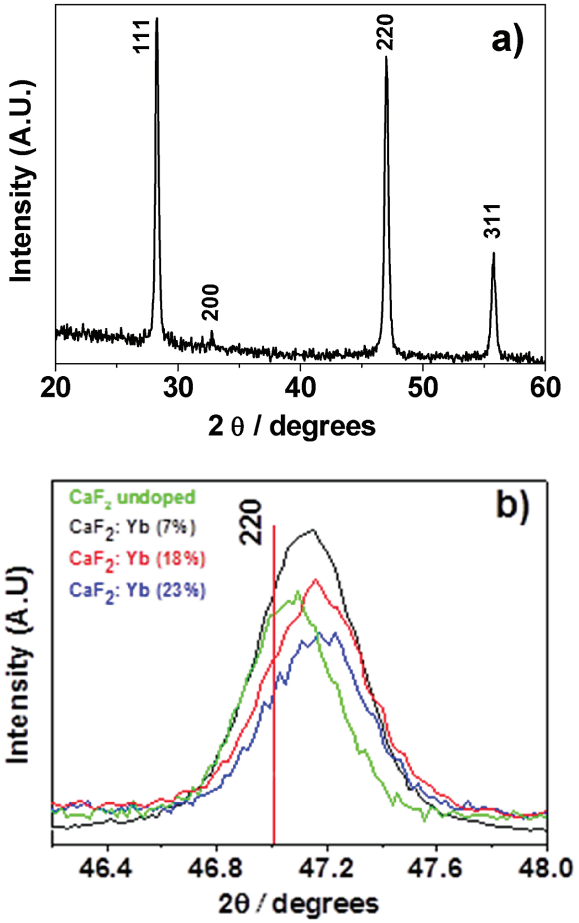

Figure 1. a) XRD pattern of the CaF_2:Yb(18%), Er(2%) film deposited at 500 °C on Si. b) A magnification of the 220 reflection of the CaF_2 films doped with different amount of Yb.

with additional fluoride ions. The lanthanide ions are supposed to substitute calcium, thus assuming an eight coordination, considering that the Ca^{2+} and Ln^{3+} ions have similar ionic radii, with Ca^{2+} = 1.12 Å and the Ln^{3+} ranging from 1.16 Å (La^{3+}) to 0.977 Å (Lu^{3+}), in eightfold coordination.[37] In particular, the Yb^{3+}, Er^{3+}, and Tm^{3+} ions have ionic radii of 0.985, 1.004, and 0.994 Å, respectively (in eightfold coordination),[37] i.e., slightly smaller than the Ca^{2+} ions. Therefore, a mere effect due to substitution of Ca^{2+} by Ln^{3+} ions gives rise to a shift toward higher 2θ angles. The *a*-axis parameters of the CaF_2:Yb, Er films and for an undoped MOCVD-grown CaF_2 film have been determined as average of all the values obtained from the individual reflections by using the relationship between *hkl* and the lattice parameter for a cubic structure, and they are reported in **Table 1** as a function of the ytterbium doping. In this context, it is worth mentioning that the *a*-axis parameter has been estimated using graphite as an internal standard (Figure S1, Supporting Information). It can be noted that the *a*-axis parameters of the doped films are slightly smaller than that of the undoped sample, and, in particular, they decrease upon increasing the ytterbium doping up to 18%. On the other hand, the 23% doped sample shows the same *a*-axis parameter of the 18% ytterbium doped CaF_2 film. The energy dispersive X-ray (EDX)

Table 1. Values of the *a*-axis parameters of the CaF_2:Yb^{3+}, Er^{3+} films grown on quartz at 500 °C.

Sample	Yb[a)] [%]	*A*-axis [Å]
CaF_2 (ICDD No. 35-816)	–	5.4630
CaF_2 film	Undoped	5.46(0)
CaF_2 film	7	5.45(3)
CaF_2 film	18	5.44(6)
CaF_2 film	23	5.44(5)

[a)]Determined by EDX.

analysis confirms that the Yb^{3+} ions are incorporated in the films, but further experiments are needed to clarify the reason of the observed similarity between the *a*-axis parameter for the two 18% and 23% ytterbium doped films. The decrease of the *a*-axis parameter may be related to the slight smaller ionic radius of Ln^{3+} vs Ca^{2+} and it clearly indicates that the lanthanide ions are incorporated in the crystalline lattice. Nevertheless, both the difference of the ionic radii of the metal ions and the effect of the charge compensation, which could be satisfied by the insertion of interstitial fluoride ions or clusters, has to be considered to explain the peak shift.

Quantitative EDX analysis confirms a uniform stoichiometry on the whole surface for all the films and for all the deposition temperatures. The EDX spectrum of a film deposited at 500 °C (**Figure 2**) shows the L and M lines of ytterbium, the K_α and K_β peaks of calcium, the K_α peak of fluorine, and the K_α peak of the silicon substrate. The erbium and thulium peaks, relative to the nominal concentration of 2%, are scarcely detectable, due to their low concentrations that are on the borderline of the detection limit of the EDX technique. It is worthy of noting the absence of C and O, whose K_α peaks should appear at 0.277 and 0.525 keV, respectively. The concentrations of the dopants, typically used for efficient UC emission,[38] of 18% of ytterbium and 2% of erbium or thulium for the CaF_2 doped films, are found through EDX in samples deposited at 500 °C. The doping amount increases upon increasing the deposition temperature and, on the contrary, decreases at temperatures lower than 500 °C. This finding may be related to a different

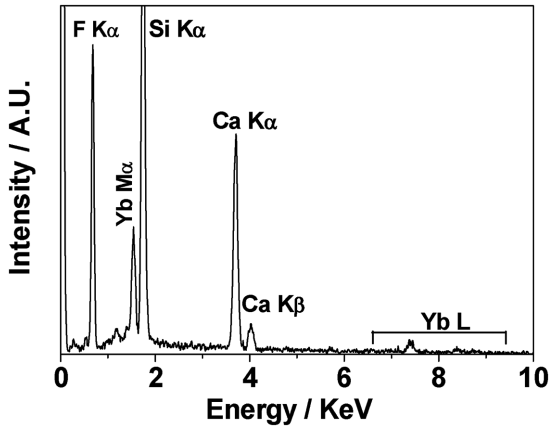

Figure 2. EDX spectrum of the CaF_2:Yb(18%), Er(2%) film deposited at 500 °C on Si (001).

decomposition behavior of the precursors, i.e., the Ca precursor likely decomposes more easily at lower temperature, so the net result is a major amount of Ca with respect to Yb, which reflects on the lower doping ratio observed at the lower temperature. Therefore, the deposition temperature permits an accurate tuning of the stoichiometry. In any case, an appropriate tuning of the mixture composition, i.e., the Ca:Ln ratio in the multicomponent source, permits the deposition of films with a desired stoichiometry at whatever temperature.

Microstructure and morphology of CaF_2 films have been studied by field emission scanning electron microscopy (FE-SEM). The FE-SEM images of the films deposited on Si (100) do not show a homogeneous surface. Film deposited at 500 °C for 90 min (Figure S2a, Supporting Information) shows some swelling, while films deposited for 60 min show a significant cracking as observed in Figure S2b (Supporting Information). These effects are likely due to the considerable difference in the thermal expansion coefficients of the CaF_2 film and that of the Si substrate. In fact, the linear thermal expansion coefficient of CaF_2 spans in the range $16.5–19.4 \times 10^{-6}$ $°C^{-1}$ versus the linear expansion coefficient of Si that is 2.6×10^{-6} $°C^{-1}$. The different behavior of swelling or cracking is essentially due to the different thickness, about 1 μm for sample reported in Figure S2a and 500 nm for the sample reported in Figure S2b. Optimization of deposition conditions, i.e., very slow cooling rate (3 °C min^{-1}) from deposition temperature to room temperature, yields almost crack-free films on Si (**Figure 3**a). In Figure 3b, the cross section of the film deposited on Si at 500 °C allows the thickness estimation of about 550 nm. Being the duration time 60 min, a growth rate of about 9–10 nm min^{-1} may be derived. The presently observed growth rate is similar to that previously reported for the deposition of pure CaF_2 from the same precursor under similar conditions.[34] FE-SEM images of films grown on glass and quartz show a smooth homogeneous surface throughout the entire 10×20 mm^2 surface. The Yb, Er co-doped CaF_2 films show crystalline grains of about 150 nm (Figure 3c,d). The CaF_2:Yb,Tm have a uniform surface with crystalline grains of about 200 nm (Figure 3e,f). The FE-SEM investigations confirm the homogeneity of the film surfaces, independently of the deposition temperature.

Upconversion measurements in the visible and near-infrared regions show that all the samples under investigation show bright luminescence upon 980 nm laser excitation. The spectra of CaF_2:Yb,Er films deposited on Si (100) substrate at 500 °C are shown in **Figure 4**a. Upon laser excitation at 980 nm, Er^{3+} emissions in the green region around 525 and 550 nm due to $^2H_{11/2} \rightarrow {}^4I_{15/2}$ and $^4S_{3/2} \rightarrow {}^4I_{15/2}$ electronic transitions, respectively, and in the red region, around 660 nm due to $^4F_{9/2} \rightarrow {}^4I_{15/2}$ transitions, indicating that $Yb^{3+} \rightarrow Er^{3+}$ UC processes are present. The complete assignments of the emission bands are reported in the caption of Figure 4 and are in perfect agreement with the bands observed in the energy level diagrams for the Er^{3+} and Yb^{3+} ions and upconversion mechanisms upon 980 nm laser excitation (Figure 4b). It is noted that the red emission is stronger than the green one so that the luminescence at the naked eyes appears to be yellow-orange. The enhancement of the red emission with respect to the green one can be ascribed to the high Yb^{3+} concentration (around 18% with respect to the total metal content) in the CaF_2 host, as also observed for

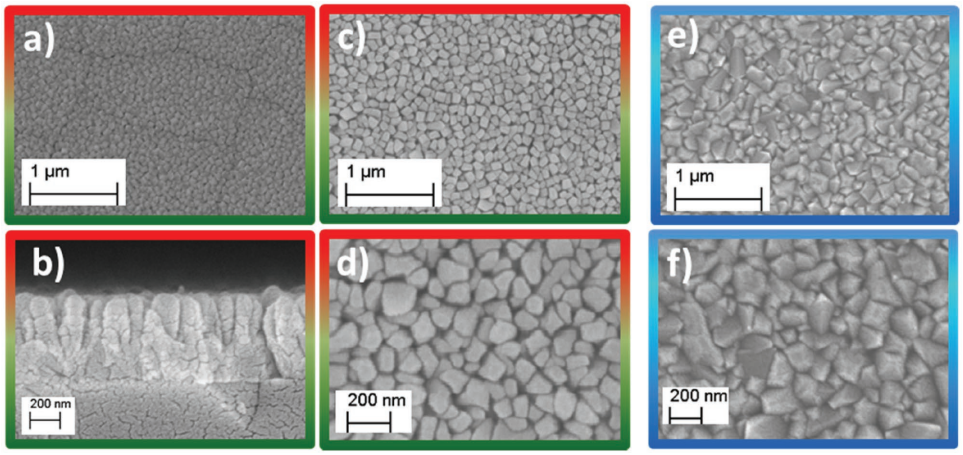

Figure 3. FE-SEM images of the CaF_2:Yb(18%), Er(2%) deposited at 500 °C: a) plan view and b) cross section of films deposited on Si (001); c) low and d) high magnification of films deposited on quartz. e) Low and f) high magnification FE-SEM images of the CaF_2:Yb(18%), Tm(2%) deposited at 500 °C on quartz.

other upconverting nanomaterials.[39] The emission spectra of the samples doped with Tm^{3+} show several bands in the UV, visible, and NIR regions, with the strongest band observed in the blue region. The upconversion properties are similar for the film deposited on Si (**Figure 5**a) or on quartz (Figure 5b). The spectrum may be assigned considering the following Tm^{3+} transitions: (I) $^1D_2 \rightarrow {}^3H_6$; (II) $^1D_2 \rightarrow {}^3F_4$; (III) $^1G_4 \rightarrow {}^3H_6$, (IV) $^1D_2 \rightarrow {}^3H_5$, (V) $^1G_4 \rightarrow {}^3F_4$, (VI) $^1G_4 \rightarrow {}^3H_5$, (VII) $^3H_4 \rightarrow {}^3H_6$. For both kinds of co-doped samples, the UC emission is clearly visible, indicating that an efficient $Yb^{3+} \rightarrow Er^{3+}$ or Tm^{3+} energy transfer is present. Some differences in the relative intensities of the Tm^{3+} emission bands are observed for samples deposited on silicon and quartz substrates, in particular for the $^1D_2 \rightarrow {}^3F_4$ and $^1G_4 \rightarrow {}^3H_6$ emission transitions. Presently, this behavior cannot be easily rationalized, and it could be tentatively attributed to an effect of cross-relaxation processes among the Tm^{3+} ions, due to possible clustering of the lanthanide ions.[40] Additional experiments using samples at different Tm^{3+} concentration would be necessary in order to shed light on this issue.

A simple process has been applied to the fabrication of CaF_2 based films, using the M(hfa)$_n$diglyme complexes, which act as single-source precursors. Deposited films are pure CaF_2 with highly homogeneous surfaces. Depending on the substrate nature further optimization may be needed to avoid cracking on Si substrates. The films show promising up conversion properties in the visible and near-infrared regions upon laser excitation for both doping mixtures. Finally, the present MOCVD approach is very challenging also in view of its easy scalability, which makes it very attractive for industrial scaling up.

Experimental Section

Film Deposition and Characterization: The films were deposited on glass, quartz, and Si (100) under low-pressure in a horizontal hot-wall reactor, in the 450–550 °C temperature range. An appropriate ratio of the Ca, Yb, and Er (or Tm) complexes were used at 120 °C, a suitable temperature for an efficient vaporization without thermal degradation. Under this condition the source is a molten mixture, since the Ca(hfa)$_2$•diglyme•H_2O and Ln(hfa)$_3$•diglyme melt in the 106–109 °C and 72–76 °C ranges, respectively. The Ln(hfa)$_3$•diglyme precursors were synthesized as previously reported in refs. [19] and [41]. Heating rates of 40 and 8 °C min^{-1} were used for the reactor chamber and the vaporization reservoir, respectively. Argon was used as a carrier gas,

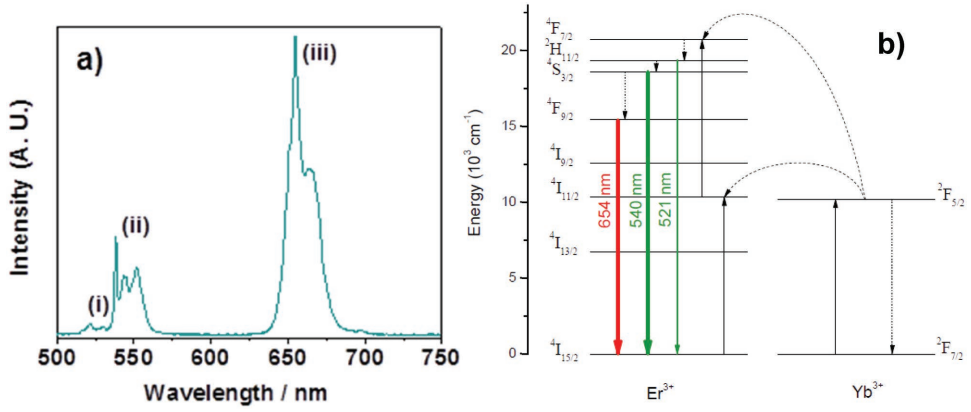

Figure 4. a) Room temperature UC emission spectrum of a CaF_2:Yb(18%), Er(2%) film deposited on Si substrate at 500 °C. The peaks correspond to the Er^{3+} transition: (I) $^2H_{1/2} \rightarrow {}^4I_{15/2}$; (II) $^4S_{3/2} \rightarrow {}^4I_{15/2}$; (III) $^4F_{9/2} \rightarrow {}^4I_{15/2}$. b) Energy level scheme for the Er^{3+} and Yb^{3+} ions and upconversion mechanisms upon 980 nm laser excitation (laser intensity 3.2 W mm^{-2}).

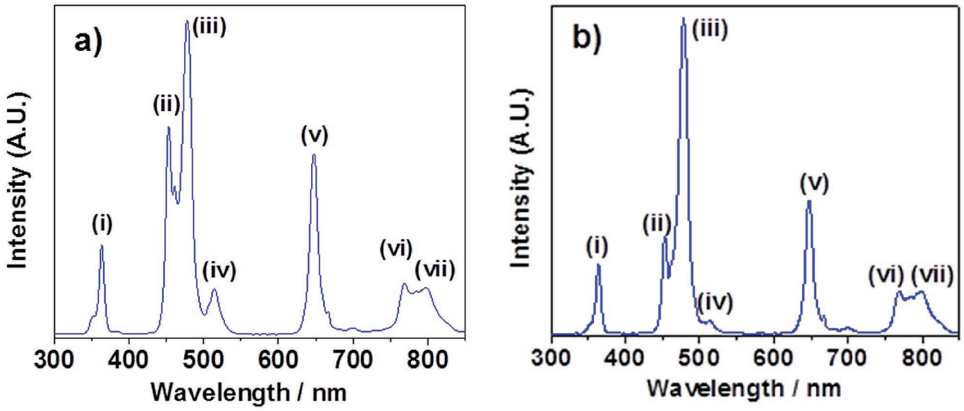

Figure 5. UC emission spectra of CaF_2:Yb(18%),Tm(2%) films deposited at 500 °C on a) Si and b) quartz substrates. The peaks correspond to the Tm^{3+} transition: (I) $^1D_2 \rightarrow {}^3H_6$; (II) $^1D_2 \rightarrow {}^3F_4$; (III) $^1G_4 \rightarrow {}^3H_6$, (IV) $^1D_2 \rightarrow {}^3H_5$, (V) $^1G_4 \rightarrow {}^3F_4$, (VI) $^1G_4 \rightarrow {}^3H_5$, (VII) $^3H_4 \rightarrow {}^3H_6$. All spectra were collected at room temperature upon 980 nm laser excitation (laser intensity of 3.2 W mm^{-2}).

while oxygen as the reactant gas was introduced in the main flow into close proximity to the reaction zone.

Film structure was analyzed by XRD in glancing incidence mode (0.5°) using a Smartlab Rigaku diffractometer, equipped with a rotating anode of Cu K_α radiation operating at 45 kV and 200 mA. Film morphology was analyzed by FE-SEM using a ZEISS SUPRA 55 VP field emission microscope. The films deposited on Si were analyzed as-dep, while films deposited on glass or quartz were Au-coated prior FE-SEM characterization. The EDX spectra were recorded using an INCA-Oxford windowless detector, having a resolution of 127 eV as the full width half maximum (FWHM) of the Mn K_α.

For the luminescence characterization, the samples were excited at 980 nm using a diode laser as the source (CNI Optoelectronics Tech), with an intensity of 3.2 W mm^{-2}. The emission spectra were detected by a Black Comet SR Spectrometer (StellarNet Inc), with optical spectral resolution of 1 nm.

Supporting Information

Supporting Information is available from the Wiley Online Library or from the author.

Acknowledgements

The authors thank the University of Catania for financial support within the FIR project and the University of Verona for funding in the frame of the "Ricerca di Base 2015" project. A.L.P. and G.M. thank Bio-nanotech Research and Innovation Tower (BRIT) laboratory of the University of Catania for the diffractometer facility.

Conflict of Interest

The authors declare no conflict of interest.

Keywords

fluorides, lanthanides, MOCVD, single precursors, upconversion films

Received: February 25, 2017
Revised: April 4, 2017
Published online: May 15, 2017

[1] C. Lorbeer, F. Behrends, J. Cybinska, H. Eckert, A. V. Mudring, *J. Mater. Chem. C* **2014**, *2*, 9439.
[2] M. Quintanilla, I. X. Cantarelli, M. Pedroni, A. Speghini, F. Vetrone, *J. Mater. Chem. C* **2015**, *3*, 3108.
[3] M. Back, R. Marin, M. Franceschin, N. Sfar Hancha, F. Enrichi, E. Trave, S. Polizzi, *J. Mater. Chem. C* **2016**, *4*, 1906.
[4] V. Mahalingam, K. N. K. B. Adusumalli, M. Koppsetti, *J. Mater. Chem. C* **2016**, *4*, 2289.
[5] P. Dolcet, A. Mambrini, M. Pedroni, A. Speghini, S. Gialanella, M. Casarin, S. Gross, *RSC Adv.* **2015**, *5*, 16302.
[6] B. Ritter, P. Haida, F. Fink, T. Krahl, K. Gawlitza, K. Rurack, E. Kemnitz, *Dalton Trans.* **2017**, *46*, 2925.
[7] J.-P. Wells, R. Reeves, *Phys. Rev. B* **2001**, *64*, 1.
[8] L. B. Su, Q. G. Wang, H. J. Li, G. Brasse, P. Camy, J. L. Doualan, A. Braud, R. Moncorge, Y. Y. Zhan, L. H. Zheng, X. B. Qian, J. Xu, *Laser Phys. Lett.* **2013**, *10*, 035804.
[9] N. N. Dong, M. Pedroni, F. Piccinelli, G. Conti, A. Sbarbati, J. E. Ramirez-Hernandez, L. M. Maestro, M. C. Iglesias-de la Cruz, F. Sanz-Rodriguez, A. Juarranz, F. Chen, F. Vetrone, J. A. Capobianco, J. G. Sole, M. Bettinelli, D. Jaque, A. Speghini, *ACS Nano* **2011**, *5*, 8665.
[10] Y. P. Du, X. Sun, Y. W. Zhang, Z. G. Yan, L. D. Sun, C. H. Yan, *Cryst. Growth Des.* **2009**, *9*, 2013.
[11] E. Kemnitz, B. Ritter, T. Krahl, K. Rurack, *J. Mater. Chem. C* **2014**, *2*, 8607.
[12] F. K. Ma, Q. Zhang, D. P. Jiang, L. B. Su, Y. J. Shao, J. Y. Wang, F. Tang, J. Xu, P. Solarz, W. Ryba-Romanowski, R. Lisiecki, B. Macalik, *Laser Phys.* **2014**, *24*, 105703.
[13] S. W. Hao, L. M. Yang, H. L. Qiu, R. W. Fan, C. H. Yang, G. Y. Chen, *Nanoscale* **2015**, *7*, 10775.
[14] P. Camy, J. L. Doualan, A. Benayad, M. von Edlinger, V. Ménard, R. Moncorgé, *Appl. Phys. B* **2007**, *89*, 539.
[15] S. Normani, A. Braud, R. Soulard, J. L. Doualan, A. Benayad, V. Menard, G. Brasse, R. Moncorge, J. P. Goossens, P. Camy, *CrystEngComm* **2016**, *18*, 9016
[16] P. Cortelletti, C. Facciotti, I. X. Cantarelli, P. Canton, M. Quintanilla, F. Vetrone, A. Speghini, M. Pedroni, *Opt. Mater.* **2017**, doi: 10.1016/j.optmat.2016.11.019.
[17] W. Y. Yin, G. Tian, W. L. Ren, L. Yan, S. Jin, Z. J. Gu, L. J. Zhou, J. Li, Y. L. Zhao, *Dalton Trans.* **2014**, *43*, 3861.
[18] G. Wang, Q. Peng, Y. Li, *J. Am. Chem. Soc.* **2009**, *131*, 14200.
[19] G. Malandrino, I. L. Fragalà, *Coord. Chem. Rev.* **2006**, *250*, 1605.
[20] N. J. Dudney, *J. Vac. Sci. Technol., A* **1998**, *16*, 615.
[21] N. Marechal, E. Quesnel, P. Juliet, Y. Pauleau, *J. Appl. Phys.* **1993**, *74*, 5203.

[22] R. K. Pandey, M. Kumar, S. A. Khan, T. Kumar, A. Tripathi, D. K. Avasthi, A. C. Pandey, *Appl. Surf. Sci.* **2014**, *289*, 77.
[23] R. J. Reeves, C. Polley, J. S. Choi, *J. Lumin.* **2009**, *129*, 1673.
[24] A. De Bonis, A. Santagata, A. Galasso, M. Sansone, R. Teghil, *Appl. Surf. Sci.* **2014**, *302*, 145.
[25] E. Daran, R. Legros, P. Pernas, C. Fontaine, *J. Appl. Phys.* **1997**, *81*, 679.
[26] C. Deiter, M. Bierkandt, A. Klust, C. Kumpf, Y. Su, O. Bunk, R. Feidenhans'l, J. Wollschläger, *Phys. Rev. B* **2010**, *82*, 085449.
[27] T. Jiang, W. Qin, F. Ding, *J. Nanosci. Nanotechnol.* **2010**, *10*, 2013.
[28] S. Nembenna, H. W. Roesky, S. Nagendran, A. Hofmeister, J. Magull, P.-J. Wilbrandt, M. Hahn, *Angew. Chem., Int. Ed.* **2007**, *46*, 2512.
[29] a) M. Ylilammi, T. Ranta-aho, *J. Electrochem. Soc.* **1994**, *141*, 1278; b) T. Pilvi, K. Arstila, M. Leskela, M. Ritala, *Chem. Mater.* **2007**, *19*, 3387.
[30] F. Meillaud, M. Boccard, G. Bugnon, M. Despeisse, S. Hänni, F.-J. Haug, J. Persoz, J.-W. Schüttauf, M. Stuckelberger, C. Ballif, *Mater. Today* **2015**, *18*, 378.
[31] M. J. Benac, A. H. Cowley, R. A. Jones, A. F. Tasch Jr., *Chem. Mater.* **1989**, *1*, 289.
[32] A. V. Blednov, O. Yu Gorbenko, S. V. Samoilenkov, V. A. Amelichev, V. A. Lebedev, K. S. Napolskii, A. R. Kaul, *Chem. Mater.* **2010**, *22*, 175.
[33] G. Malandrino, F. Castelli, I. L. Fragala', *Inorg. Chim. Acta* **1994**, *224*, 203.
[34] A. M. Makarevich, A. S. Shchukin, A. V. Markelov, S. V. Samoilenkov, P. P. Semyannikov, N. P. Kuzmina, *ECS Trans.* **2009**, *25*, 525.
[35] A. M. Makarevich, P. P. Semyannikov, N. P. Kuzmina, *Russian J. Inorg. Chem.* **2010**, *55*, 1940.
[36] N. P. Kuzmina, D. M. Tsymbarenko, I. E. Korsakov, Z. A. Starikova, K. A. Lysenko, O. V. Boytsova, A. V. Mironov, I. P. Malkerova, A. S. Alikhanyan, *Polyhedron* **2008**, *27*, 2811.
[37] R. D. Shannon, *Acta Crystallogr. Sect. A* **1976**, *32*, 751.
[38] J. Zhou, Q. Liu, W. Feng, Y. Sun, F. Li, *Chem. Rev.* **2015**, *115*, 395.
[39] J. A. Capobianco, F. Vetrone, J. C. Boyer, A. Speghini, M. Bettinelli, *J. Phys. Chem. B* **2002**, *106*, 1181.
[40] P. Villanueva-Delgado, K. W. Kramer, R. Valiente, M. de Jong, A. Meijerink, *Phys. Chem. Chem. Phys.* **2016**, *18*, 27396.
[41] A. Valore, E. Cariati, S. Righetto, D. Roberto, F. Tessore, R. Ugo, I. L. Fragalà, M. E. Fragalà, G. Malandrino, F. De Angelis, L. Belpassi, I. Ledoux-Rak, K. Hoang Thi, J. Zyss, *J. Am. Chem. Soc.* **2010**, *132*, 4966.

